Journal of the European Ceramic Society 21 (2001) 2895–2902

www.elsevier.com/locate/jeurceramsoc

Microstructural evolution in nanocrystalline Y–TZP containing a silicate glass

Ramasamy Ramamoorthy [1], Rachman Chaim *

Department of Materials Engineering, Technion-Israel Institute of Technology, Haifa 32000, Israel

Received 25 November 2000; accepted 20 January 2001

Abstract

Nanocrystalline yttria stabilized tetragonal zirconia polycrystal (NC–Y–TZP) powders were coated with a sodium strontium silicate glass using the sol-gel technique. The compact powders were sintered at 1400°C for 1 h resulting in dense nanocrystalline pellets with 5, 10 and 15 vol.% glass. Short pre-sintering heat treatment at 800°C caused the full stabilization of the tetragonal phase while long treatments led to the devitrification of the glassy phase. The mean grain size decreased from 196 nm in the glass-free specimen to 140, 110 and 100 nm in the specimens containing 5, 10 and 15 vol.% glass, respectively. The grain size distribution width also decreased with increase in the glass content. TEM revealed the morphological changes of the highly facetted polyhedral grains in the glass-free specimens into the round-shape grains with increase in the glass content. The effect of the glass on the phase formation, densification and microstructure have been discussed.

Keywords: Glassy phase; Microstructure; Nanoparticles; Sol-gel processes; Y-TZP; ZrO_2

1. Introduction

Yttria-stabilized tetragonal zirconia polycrystals (Y–TZP) is among the high strength ceramics used for structural components. It has been demonstrated that submicron grained Y–TZP can be deformed superplastically at temperatures around 1300°C.[1–3] The underlying mechanical phenomenon of superplastic forming in the nanocrystalline (NC) ceramics has shown a new direction of joining ceramic bodies at relatively low temperatures.[4,5] The microstructural parameters such as fine grain size and grain boundary composition are considered to enhance the superplastic deformation behavior. Apparently, the extensive ductility of the Y–TZP ceramics is a consequence of their grain size stability during the high temperature deformation. In impure ceramics high creep deformations may be achieved by viscous flow of the grain boundary (gb) glassy phases.[6,7] This was the original motivation for introducing a glassy phase into the ceramics in a controlled manner[8–16] in order to benefit from their enhanced flow properties.

Even though the grain size refinement was found to lower the superplastic forming temperature and stress, or increase the strain rate, the nanocrystalline ceramics were not found to exhibit the expected improvement of several orders of magnitude in the strain rate.[17–19] However, the high volume fraction of the grain boundaries in the nanostructured ceramics wetted by the grain boundary glassy phase may improve the superplastic forming ability of the nanostructured ceramic body.[20] Nevertheless, the final sintered microstructure and the grain boundary glassy phase distribution have significant effects on the plastic behavior and thus should be characterized.

Incorporation of the glassy phase into the grain boundaries may be performed by coating the powder particles with the glass through the sol-gel technique.[21,22] Assuming a coating thickness of 1 nm on an initial particle with 20 nm in diameter, the estimated volume fraction of the glass is about 10%.[23] Thus 5, 10 and 15 vol.% glass contents were applied in the present nanocrsyatlline powders. The microstructural modification of the NC–Y–TZP grains with respect to the presence of the grain boundary glassy phase were investigated and the effect of the glass on the densification behavior is reported.

* Corresponding author. Tel.: +972-4-8294589; fax: +972-4-8321978.

E-mail address: rchaim@tx.technion.ac.il (R. Chaim).

[1] Present address: Process and Aerosol Measurement Technology, Bismarckstrsse 81, Universität Duisburg, 47048 Duisburg, Germany.

0955-2219/01/$ - see front matter
PII: S0955-2219(01)00215-1

2. Experimental procedures

Commercial nanocrystalline Y–TZP powder (Tioxide) was used as the core material in this study. This powder was coated by the strontium sodium silicate glass through the sol-gel method. An ethanol–water solution corresponding to an initial composition (mol%) of 80% SiO_2–15% Na_2O–5% SrO (SNS) was prepared by dissolving silicon tetrachloride ($SiCl_4$) in ethanol and sodium nitrate ($NaNO_3$) and strontium nitrate $Sr(NO_3)_2$ in water. However, the sodium content of the resultant precipitate was found by chemical wet analysis to deviate strongly from the nominal composition. The final composition of the glass was found as 93% SiO_2–6% SrO–1% Na_2O. Appropriate amounts of this solution were added to the dispersion of the nanocrystalline Y–TZP powder in distilled water in order to reach the glass concentrations of 5, 10 and 15 vol.%. The dispersion of the NC–Y–TZP within the glass solutions were ultrasonically mixed for 10 min. Deposition of the glass took place by adding diluted ammonium hydroxide into the solution. The resultant slurry was stirred using a magnetic stirrer and simultaneously heated for a period of 12 h to dryness. Then the powder was gently ground in an agate mortar and annealed at 600°C for 1 h.

The uncoated and the glass-coated NC–Y–TZP powders were compacted into cylinderical pellets of 15 mm×15 mm, uniaxially pressed at 20 MPa, followed by cold isostatic pressing at 250 MPa. The relative green density was measured through weighing to be ~55%. The compacts were fired at 800°C for 3 h and sintered at 1400°C for 1 h. The pre-sintering heat treatment was performed to form fully tetragonal phase in the glass-doped specimens. The density of the sintered compacts were measured by the Archimedes technique; the density of the glass was taken into account while determining the theoretical density of each specimen. The phase content was determined using X-ray diffractometer (PW-3020) equipped with copper K_α radiation. The microstructure was studied using SEM (XL30) and TEM (2000FX) combined with X-ray energy dispersive spectroscopy (EDS). The sintered specimens were polished and thermally etched for SEM observations. The TEM specimens were prepared by the conventional techniques. The morphology of the NC–Y–TZP powder particles coated with the glass was also observed in TEM by dispersing the powder onto a carbon coated copper grid.

3. Results

The as-received nanocrystalline powder was composed of elongated polyhedron-shaped crystallites (Fig. 1a). The two perpendicular diameters (C and A) in TEM images were used to establish the normal crystallite (particle) size distribution in this powder (Fig. 1b);

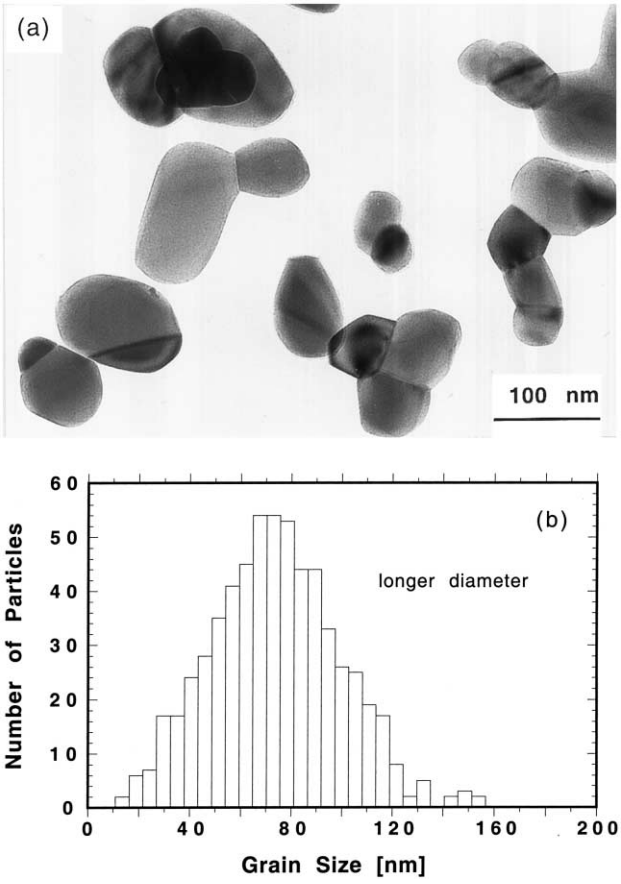

Fig. 1. (a) TEM image of the as-received NC zirconia powder. (b) normal particle size distribution of the longer diameter of the powder particles.

the mean particle sizes (diameter) in each direction were 73 and 50 nm, respectively. The aspect ratio (C/A) of the crystallites varied in the range of 1.4–1.7. X-ray diffraction spectrum of the powder (Fig. 2a) exhibited mainly monoclinic phase peaks with a few percent of the tetragonal phase. This finding is in agreement with the powder character that is a mechanical mixture of pure nanocrystalline monoclinic zirconia and cubic yttria.

TEM image of the NC–Y–TZP particles coated with 10 vol.% SNS glass (i.e. Fig. 3a) and annealed at 600°C exhibited a uniform coating of the glass over the particle surfaces. The thickness of the glassy layer was fairly homogeneous over the praticles but varied between 3 and 6 nm in different particles. The distribution of the glass was not uniform in the powders coated with 5 and 15 vol.% SNS glass; some uncoated particles as well as glass pockets were observed along with the NC–Y–TZP particles (Fig. 3b). Tilting experiments in TEM confirmed the amorphous nature of the coating layer and the glass pockets. The coating process followed by the annealing heat treatment at 600°C did not change the phase content of the precursor powder.

Different powder compacts sintered at 1400°C for 1 h (without the pre-sintering heat treatment) were nearly

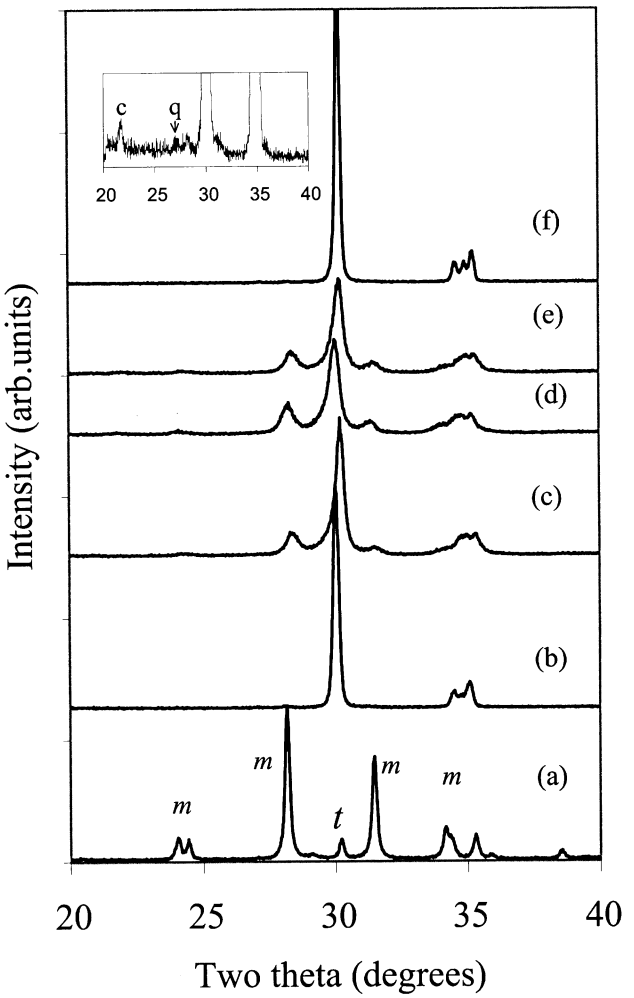

Fig. 2. X-ray diffraction spectra of (a) NC–Y–TZP powder; (b) glass-free; (c) 5 vol.% SNS glass; (d) 10 vol.% SNS glass; (e) 15 vol.% SNS glass compacts sintered at 1400°C for 1 h. (f) 10 Vol.% SNS glass compact presintered at 800°C for 3 h followed by sintering at 1400°C for 1 h. "c" And "q" in the inset refer to cristobalite and quartz, respectively.

fully dense, 98–99% of their theoretical densities (Table 1). This sintering condition led to full stabilization of the tetragonal phase (Fig. 2b) in the glass-free NC–Y–TZP. At similar sintering conditions, the glass-containing specimens exhibited a considerable fraction of the monoclinic phase along with the tetragonal phase (Figs. 2c, d and e). The monoclinic phase content was highest in the 10 vol.% glass specimens (Table 1). However, pre-sintering heat treatment at 800°C for about 3 h led to the transformation of the monoclinic phase into the tetragonal symmetry (compare Fig. 2d and f). Such a heat treatment did not change the amorphous nature of the glassy phase. Nevertheless, similar pre-sintering heat treatment for a prolonged period (above 10 h) caused the devitrification of the glass into cristobalite and quartz forms (the inset in Fig. 2).

The effect of the glass content on the microstructure of the sintered NC–Y–TZP specimens, as well as their grain size and distribution are shown in Figs. 4 and 5,

Table 1
Characteristics of the NC–Y–TZP specimens sintered at 1400°C for 1 h

Glass content (vol.%)	Relative density (%)	Theoretical density (g/cm^3)	Phase t	Content (%)[a] m	Maximum linear shrinkage (%)[b]
0	98	5.98	100	–	16.25
5	99	5.85	83	17	17.25
10	98	5.65	69	31	16.80
15	99	5.56	74	26	17.47

[a] t And m refer to tetragonal and monoclinic polymorphs, respectively.
[b] Up to 1400°C.

respectively. The grain size in the glass-free specimen varied from 100 to 600 nm (Fig. 4a), with wide log-normal distribution (Fig. 5a). However, a few larger grains of about 1 μm were also observed. The overall microstructure of the NC–Y–TZP specimens was refined by the presence of the glass as shown in Fig. 4. Moreover, increase in the volume fraction of the glass was accompanied by narrowing of the grain size distribution widths as well as by a decrease in the mean grain size (Figs. 5b–d) compared to that of the glass-free specimen. The average grain size decreased from 196 nm in the glass-free specimen to 140, 110 and 99 nm in the 5, 10 and 15% glass specimens, respectively. However, a few grains larger than 500 nm were also observed (Fig. 4c and d) the number of which was found to increase with the increase in the glass content.

The morphological changes of the NC–Y–TZP particles in the sintered compacts due to the glass addition were well resolved in the TEM images shown in Fig. 6. A gradual modification of the particle shape and the internal microstructure were observed with the increase in the volume fraction of the glass. The highly faceted polyhedral grains in the glass-free specimens were gradually converted into round-shaped spherical grains in the glass-containing specimens, in an increasing manner.

In support of the microstructural observations in the glass-containing specimens, the EDS microananlysis revealed the presence of the glass along the grain boundaries and the grain junctions. The composition of the glass-coated particles as well as the overall composition of the sintered specimens are shown in Table 2. The observed sodium content was below the detection limit of the technique (0.2%) and thus was neglected. Silicon and strontium were found in all the glassy-phase regions. Generally, the glass content on the coated powder particles was about or below 5 wt.%, regardless of the composition of the powder specimen. This effect may be associated with the segregation of the glass to form glass chunks, the effect of which increased as the glass content increased. The Y_2O_3 content in these powders varied between 2.5 and 4.5 wt.%. This effect should be attributed to the powder characteristics which is a mechanical mixture of pure nanocrystalline ZrO_2

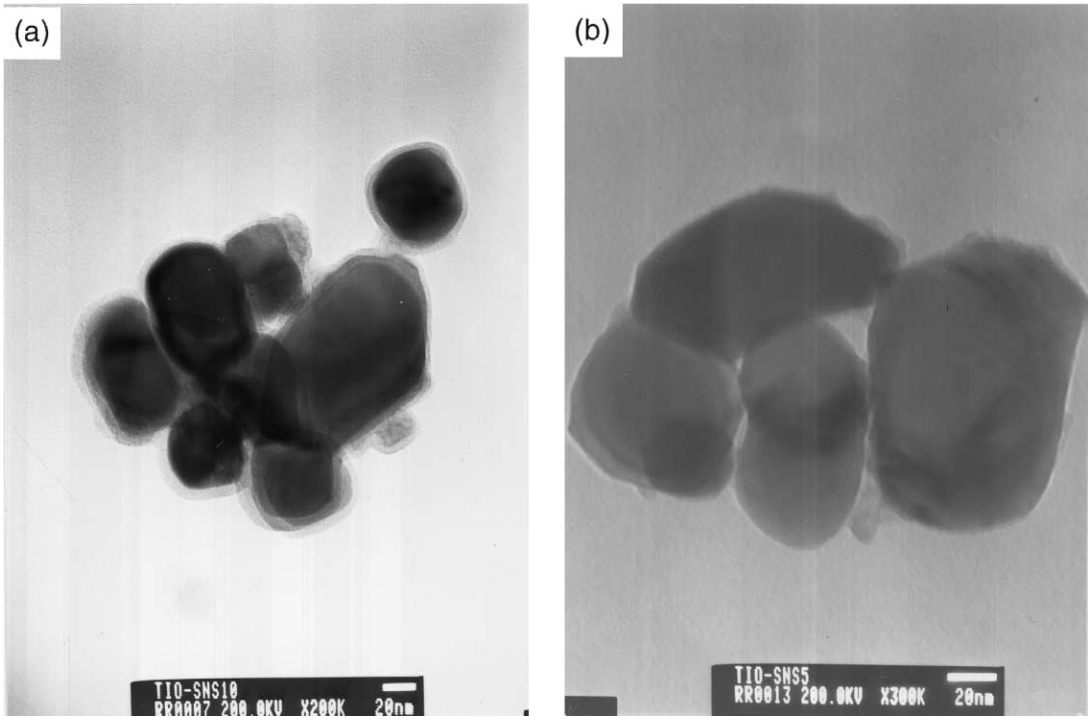

Fig. 3. TEM images of the NC–Y–TZP powder coated with (a) 10 vol.% SNS glass, and (b) 5 vol.% SNS glass.

and Y_2O_3. Thus, the large variation in the Y_2O_3 composition is a manifestation of its partial dissolution, aided by the glass at 600°C. Nevertheless, the Y_2O_3 composition in the sintered specimens was higher and around 4 wt.%, close to the powder designated composition. In the specimens sintered at 1400°C for 1 h (not shown in Table 2), the SiO_2/SrO ratio varied from 0.15 to 1 inverse to that expected for the glass composition. It should be noted that the overlap between the weak Si–K peak and the strong Zr–L peak resulted in underestimation of the Si content during the data processing. However, pre-sintering at 800°C for 3 h prior to the final sintering at 1400°C for 1 h resulted in higher SiO_2/SrO ratios (2.5–12.6). Apparently, the latter pre-sintering at elevated temperature enhanced the compositional homogenization of the glassy phase.

4. Discussion

The tetragonal to monoclinic phase transformation temperature in the ZrO_2–SiO_2 binary oxides formed by the sol-gel technique was found to increase with the increase in the SiO_2 content.[24] This tetragonal stability in SiO_2-rich compositions was related to inhibited diffusion of the Zr through the SiO_2 matrix, which in turn retarded the nucleation and growth of the zirconia grains. However, using FTIR technique, the tetragonal stability in ZrO_2-rich compositions (>90%) was related to the formation of strong Si–O–Zr bonds at the ZrO_2/SiO_2 interfaces.[25] Nevertheless, these bonds disappeared above 1000°C. The presence of the SNS glass in the present powder compacts was found to decrease the tetragonal phase content after sintering at 1400°C. The present dilatometric shrinkage data (Table 1) indicated that densification may be enhanced by the presence of the glassy phase. On the other hand, finer grains were resulted in the glass-containing specimens relative to the glass-free specimens. Therefore, densification is most probably enhanced at the initial sintering stages by particle rearrangement aided by the viscous glass, and latter by limited diffusion through the glass. In this respect, the glassy layer which surrounds the zirconia particles may act as a diffusion barrier both for Zr and Y cations, hence inhibit the grain growth. Uchikoshi et al. [26] reported on hindrance of grain growth but also of densification in Y–TZP doped with SiO_2 contents above 0.3 wt.%. Their examinations, however, were limited to the SiO_2 contents of up to 1 wt.% only.

In addition to the low Y_2O_3 content of the NC–Y–TZP, some part of the yttria might have dissolved in the glass, thus decreasing the tetragonal phase stability. The fraction of the monoclinic phase increased as the glass content increased from 5 to 10%. However, in the 15% glass specimen, the monoclinic phase content decreased again (i.e. lower than that in the 10% glass specimen). This trend could be understood by refering to the equilibrium thickness of the grain boundary glassy phase in ceramics. The thermodynamic trend of the intergranular glassy phase to adopt an equilibrium thickness was discussed by

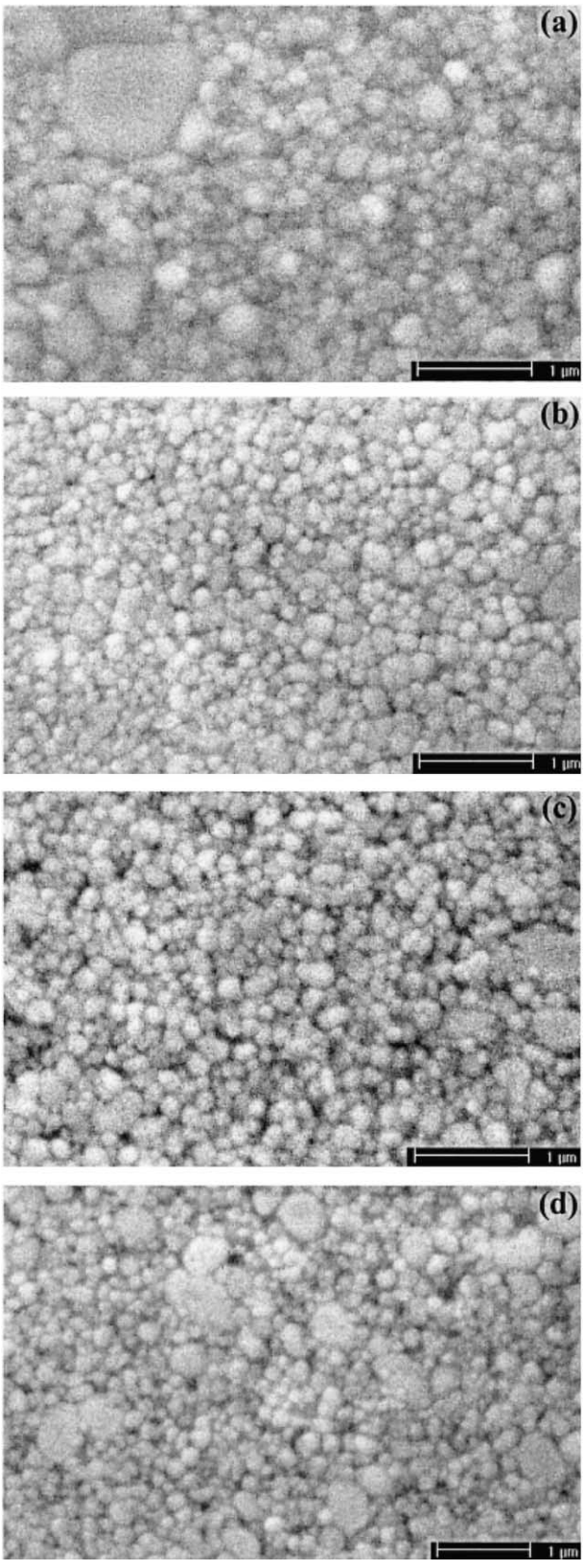

Fig. 4. SEM images of the NC–Y–TZP specimens sintered at 1400°C for 1 h: (a) glass-free; (b) 5 vol.% SNS glass; (c) 10 vol.% SNS glass; (d) 15 vol.% SNS glass.

Clarke.[27] This leads to an optimum in the volume fraction of the glassy phase for a given grain size in the nanometer regime, if all the glass should be located at the grain boundaries. The excess glass, above this volume fraction, may segregate to form glassy phase pockets. Such glass pockets are less effective both in enhancing densification and inducing the constrained effect as well as affecting the diffusion phenomenon. In this respect, expulsion of the glassy phase during the grain growth in liquid phase sintered zirconia ceramics were reported.[28]

The relatively constant thickness of the glassy phase coating on the particle surfaces was indicative for full wetting of the NC–Y–TZP surfaces at elevated temperatures. Similar SiO_2 coatings that were formed on the Y–TZP powders through the sol-gel technique were 1.6 nm thick and remained amorphous up to 1200°C.[29] Full wetting is a characteristic requirement for better superplastic formability of the dense specimens. However, Sakuma et al., [13,16,30] reported of the presence of the amorphous phase at the grain boundary corners but not at the grain boundary surfaces, in the dense specimen. They also found that the Y–TZP grain growth was inhibited by the presence of the glassy phase in the temperature range of 1400–1800°C. On the other hand, segregation of SiO_2, even at very low concentrations (i.e. 120 ppm) into the zirconia grain boundaries in ZrO_2–8 wt.% Y_2O_3 alloys were reported using SIMS maps.[31] Both the experimental and the calculated ZrO_2–SiO_2 phase diagrams exhibit negligible solid solubility between the two oxides.[32] However, using in situ transmission electron microscopy, Ikuhara et al.[33] have shown surface dissolution of the SiO_2 in ZrO_2 above 1300°C and SiO_2 reprecipitation by cooling below 1300°C. Thus, the limited solubility of the SNS glass and the Y–TZP grains is expected to aid only to a limited extent the liquid phase sintering, and thereby retard the grain growth.

The microstructural changes due to the presence of the glass were well observed in the SEM and TEM images. The inter-granular glassy phase was represented by diluteness of the Y–TZP particles and their spherical shape. It has been clearly shown (Fig. 6) that the extent of the microstructural changes depended on the volume fraction of the glass. As the glass content increased from 5% via 10 and 15%, a gradual modification of the particle shape and distribution was noticed. The facetted, polyhedral and anisotropically shaped grains in the glass-free Y–TZP were found to be well contrasted with round-shape and equiaxed particles in the 5, 10 and 15% glass-containing specimens, in an increasing manner. Thus, physically, the relative amount of the glassy phase influences the dihedral angle between the grains. This angle varies from 100–130° in the glass-free specimen, whereas it decreases to less than 90° in the 5% glass specimen and further decreases to zero in the 15%

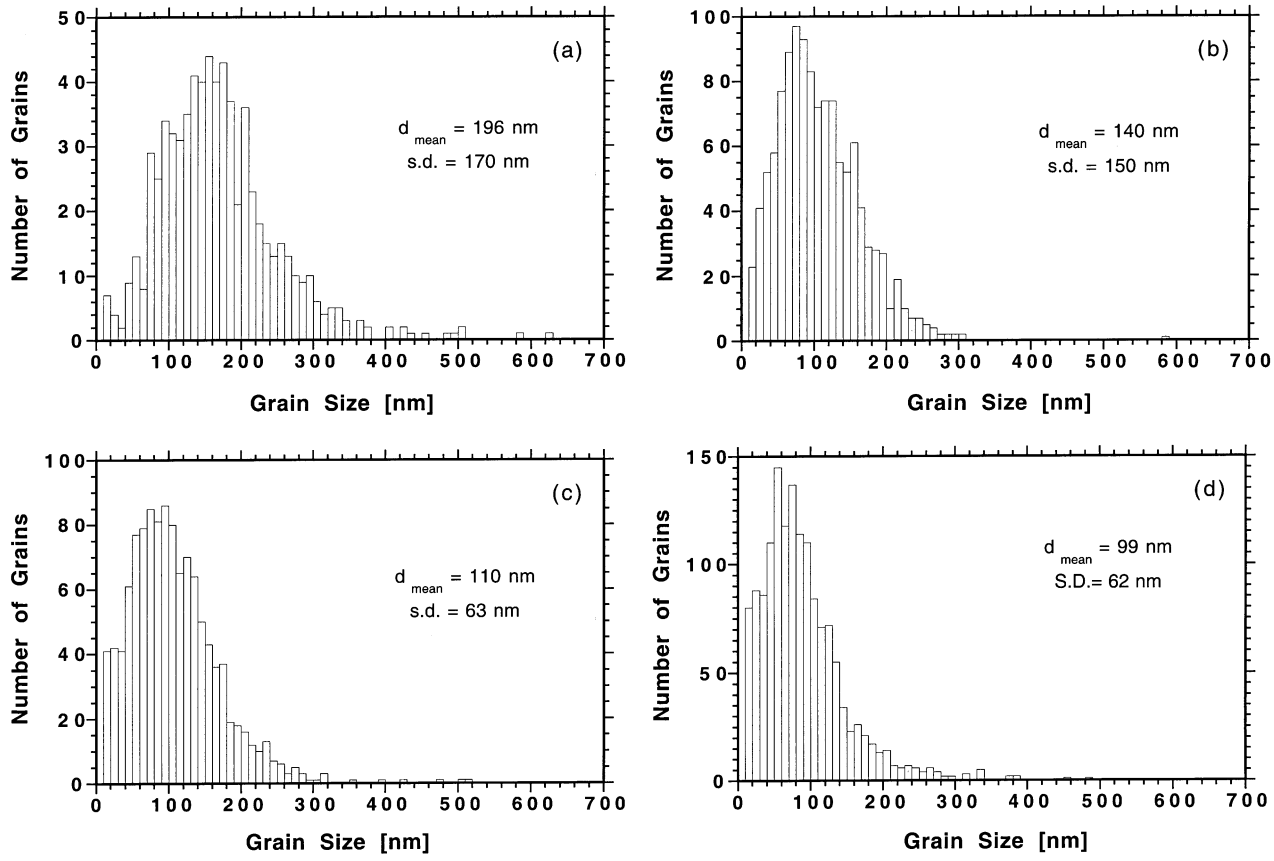

Fig. 5. Grain size distribution in the sintered NC–Y–TZP specimens: (a) glass-free; (b) 5 vol.% SNS glass; (c) 10 vol.% SNS glass; (d) 15 vol.% SNS glass.

Table 2
Composition of the glass-coated NC–Y–TZP powders and dense specimens

Glass content (vol.%)	Coated particles (wt.%)				Sintered (800 + 1400°C) (wt.%)			
	ZrO_2	Y_2O_3	SiO_2	SrO	ZrO_2	Y_2O_3	SiO_2	SrO
0	*[a]				93.83	6.09	–	–
5	91.21	4.43	3.09	1.27	92.56	3.68	2.69	1.07
	92.53	2.26	3.88	1.33	93.13	3.85	2.15	0.87
10	95.03	2.49	1.10	1.38	92.52	3.38	3.70	0.40
	95.27	2.62	0.89	1.22				
15	93.86	3.12	1.80	1.22	90.80	3.61	5.18	0.41
	94.86	2.87	0.87	1.40	90.11	3.78	6.11	–

[a] Mechanical mixture of pure nanocrystalline ZrO_2 and Y_2O_3 powders.

glass specimen. This is an indication that the grain boundaries are completely wetted by the inter-granular glassy phase.[15] del Monte et al.[24] related the polyhedral and ellipsoidal shaped zirconia grains in the ZrO_2–SiO_2 system to the monoclinic and tetragonal polymorphs, respectively. This shape change was attributed to the homogeneous strain induced by the silica matrix on the tetragonal grains, hence the stability of the tetragonal phase due to the constrained effects. Similar morphological changes were observed by Zhao et al.[30] in silica-doped Y–TZP ceramics.

The glassy phase in the present nanocrystalline ceramics acts as an interconnected feature of the microstructure. Such a continuous three dimensionally interconnected second phase can be a short circuit transport path by viscous flow during the plastic deformation of the polycrystals.[30] It is evident that the effectiveness of the glassy phase in supplying continuous superplastic

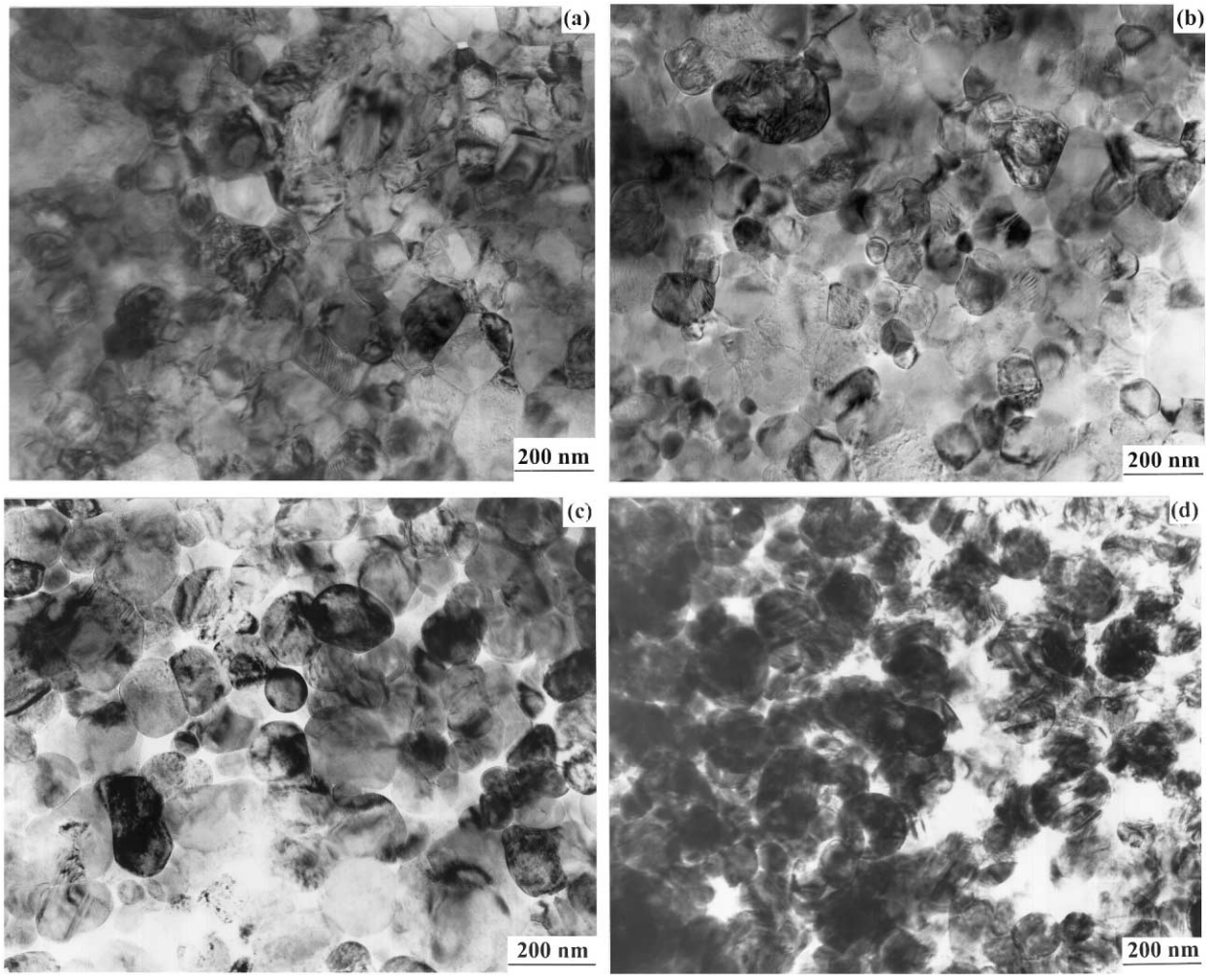

Fig. 6. TEM images showing the morphological and microstructural changes in the zirconia grains with increase in the glass content: (a) glass-free; (b) 5 vol.% SNS glass; (c) 10 vol.% SNS glass; (d) 15 vol.% SNS glass.

strains depends also on its rheological properties, and these deserve further investigation.

5. Conclusions

Sodium strontium silicate glass was coated over the NC–Y–TZP nanoparticles in three different concentrations by the sol-gel technique. The extent of the microstructural changes was dependent on the volume fraction of the glass. The sintered microstructure of the glass-doped specimens became finer with increase in the glass content relative to the glass-free specimen. The glass-free specimens contained facetted polyhedral grains with a wide grain size distribution while their glass-doped counterparts composed of rounded grains with narrower grain size distributions. The observed inhibition of the grain growth in the glass-doped specimens was related to limited diffusion of the cations through the grain boundary glassy phase. The inter-granular glassy phase is well represented by the narrowness of the grain size distribution and its spherical shape. The dihedral angle between the zirconia grains and the glassy phase was below 90° in the 5 vol.% glass and decreased to zero in the 15 vol.% glass-doped specimens, compared to 100–130° in the glass-free specimens. This is the clear indication for the complete wetting of the grain boundaries by the glassy phase.

Acknowledgements

The authors thank the Israel Ministry of Science, Culture and Sports for supporting this research through the infrastructure grant No. 1090-1-98. This research was partially supported by the Fund for the Promotion of research at the Technion.

References

1. Wakai, F., Skaguchi, S. and Matsuno, Y., Superplasticity of yttria-stabilized tetragonal ZrO_2 polycrystals. *Adv. Ceram. Mater.*, 1986, **1**, 259–263.

2. Nieh, T. G., McNally, C. M. and Wadsworth, J., Superplastic behavior of a yttria-stabilized tetragonal xirconia polycrystal. *Scripta metall.*, 1988, **22**, 1297–1300.
3. Nieh, T. G., Wadsworth, J. and Sherby, O. D., *Superplasticity in metals and ceramics*. Cambridge Solid State Science Series, Cambridge, 1997 pp. 91–99.
4. Gutierrez-Mora, F., Dominguez-Rodriguez, A., Routbort, J. L., Chaim, R. and Guiberteau, F., Joining of yttria-tetragonal stabilized zirconia polycrystals using nanocrystals. *Scripta Mater.*, 1999, **41**, 455–460.
5. Chaim, R. and Ravi, B. G., Joining of alumina ceramics using nanocrystalline tape cast interlayers. *J. Mater. Res.*, 2000, **15**, 1724–1729.
6. Pharr, G. M. and Ashby, M. F., On creep enhanced by a liquid phase. *Acta metall.*, 1983, **31**, 129–138.
7. Dryden, J. R., Kucerovsky, D., Wilkinson, D. S. and Watt, D. F., Creep deformation due to a viscous grain boundary phase. *Acta Metall.*, 1989, **37**, 2007–2015.
8. Hwang, C.-M.J. and Chen, I.-W., Effect of a liquid phase on superplasticity of 2-mol%–Y_2O_3-stabilized tetragonal zirconia polycrystals. *J. Am. Ceram. Soc.*, 1990, **73**, 1626–1632.
9. Yoshizawa, Y.-I. and Sakuma, T., Role of grain-boundary glass phase on the superplastic deformation of tetragonal zirconia polycrystal. *J. Am. Ceram. Soc.*, 1990, **73**, 3069–3073.
10. Gust, M., Goo, G., Wolfenstine, J. and Mecartney, M. L., Influence of amorphous grain boundary phases on the superplastic behavior of 3-mol.%-yttria-stabilized tetragonal zirconia polycrystals (3Y-TZP). *J. Am. Ceram. Soc.*, 1993, **76**, 1681–1690.
11. Rouxel, T. and Wakai, F., The brittle to ductile transition in a Si_3N_4/SiC composite with a glassy grain boundary phase. *Acta Metall. Mater.*, 1993, **41**, 3203–3213.
12. Seidensticker, J. R. and Mayo, M. J., *Scripta Metall. Mater.*, 1994, **31**, 1749–1754.
13. Kajihara, K., Yoshizawa, Y. and Sakuma, T., The enhancement of superplastic flow in tetragonal zirconia polycrystals with SiO2-doping. *Acta Metall. Mater.*, 1995, **43**, 1235–1242.
14. Shi, J. L., Zhu, G. Q. and Lai, T. R., Compressive deformation behaviour of superplastic Y-TZP based ceramics: Role of grain boundary phases. *J. Eur. Ceram. Soc.*, 1997, **17**, 851–858.
15. Tekeli, S. and Davies, T. I., Influence of a transition metal oxide (CuO) on the superplastic behaviour of 8 mol.% yttria-stabilised cubic zirconia polycrystal (8Y-CSZ). *J. Mater. Sci.*, 1998, **33**, 3267–3273.
16. Thavorniti, P., Ikuhara, Y. and Sakuma, T., Microstructural characterization of superplastic SiO_2-doped TZP with a small amount of oxide addition. *J. Am. Ceram. Soc.*, 1998, **81**, 2927–2932.
17. Chen, L., Rouxel, T., Chaim, R., Vesteghem, H., Sherman, D.;Superplasticity and creep in monoclinic, Y-PSZnano-grainedzirconia, *Mater. Sci. Forum*, 1997, **243-245**, 245–250.
18. Jimenez-Melendo, M., Dominguez-Rodriguez, A. and Bravo-Leon, A., Superplastic flow of fine-grained yttria-stabilized zirconia polycrystals: constitutive equation and deformation mechanisms. *J. Am. Ceram. Soc.*, 1998, **81**, 2761–2776.
19. Gutierrez-Mora, F., Dominguez-Rodriguez, A., Jimenez-Melendo, M., Chaim, R. and Hefetz, M., Creep of nanocrystalline Y-SZP ceramics. *NanoStruct. Mater.*, 1999, **11**, 531–537.
20. Chaim, R., Plastic deformation in impure nanocrystalline ceramics. *J. Mater. Res.*, 1999, **14**, 2508–2517.
21. Nakajima, A. and Messing, G. L., Liquid-phase sintering of alumina coated with magnesium aluminosilicate glass. *J. Am. Ceram. Soc.*, 1998, **81**, 1163–1172.
22. Kong, Y.-M., Kim, S., Kim, H.-E. and Lee, I.-S., Reinforcement of hyroxyapatite biocermic by addition of ZrO_2 coated with Al_2O_3. *J. Am. Ceram. Soc.*, 1999, **82**, 2963–2968.
23. Chaim, R., Percolative composite model for prediction of the properties of nanocrystalline materials. *J. Mater. Res.*, 1997, **12**, 1828–1836.
24. del Monte, F., Larsen, W. and Mackenzie, J. D., Stabilization of tetragonal ZrO_2 in ZrO_2–SiO_2 binary oxides. *J. Am. Ceram. Soc.*, 2000, **83**, 628–634.
25. del Monte, F., Larsen, W. and Mackenzie, J. D., Chemical interactions promoting the ZrO_2 tetragonal stabilization in ZrO_2-SiO_2 binary oxides. *J. Am. Ceram. Soc.*, 2000, **83**, 1506–1512.
26. Uchikoshi, T., Sakka, Y., Ozawa, K. and Hiraga, K., Preparation and sintering of silica- doped zirconia by colloidal processing. *MRS Symp. Proc.*, 1997, **457**, 33–38.
27. Clarke, D. R., On the equilibrium thickness of intergranular glass phases in ceramic materials. *J. Am. Ceram. Soc.*, 1987, **70**, 15–22.
28. De Souza, D. P. F. and De Souza, M. F., Liquid phase sintering of RE_2O_3: YSZ ceramics, Part I: Grain growth and expelling of the grain boundary glass phase. *J. Mater. Sci.*, 1999, **34**, 4023–4030.
29. Wang, S. W., Huang, X. X., Guo, J. K. and Li, B. S., Synthesis and characterization of yttria-stabilized tetragonal zirconia polycrystalline powder coated with silica layers. *Mater. Lett.*, 1996, **28**, 43–46.
30. Zhao, J., Ikuhara, Y. and Sakuma, T., Grain growth of silica-added zirconia annealed in the cubic/tetragonal two-phase region. *J. Am. Ceram. Soc.*, 1998, **81**, 2087–2092.
31. Lee, J.-H., Mori, T., Li, J.-G., Ikegami, J.-G., Komatsu, M. and Haneda, H., Imaging secondary-ion mass spectroscopy observation of the scavenging of siliceous film from 8-mol%-yttria-stabilized zirconia by the addition of alumina. *J. Am. Ceram. Soc.*, 2000, **83**, 1273–1275.
32. *Phase Diagrams for Zirconium+Zirconia Systems*, ed. H. M. Ondik and H. F. McMurdie. The ACS and NIST, Westerville, Ohio, 1998, p. 134.
33. Ikuhara, Y., Nagai, Y., Yamamoto, T. and Sakuma, T., High-temperature behavior of SiO_2 at grain boundaries in TZP. *Interface Sci.*, 1999, **7**, 77–84.